

# PHYSICAL REVIEW B

## CONDENSED MATTER AND MATERIALS PHYSICS

THIRD SERIES, VOLUME 61, NUMBER 4

15 JANUARY 2000-II

### RAPID COMMUNICATIONS

*Rapid Communications are intended for the accelerated publication of important new results and are therefore given priority treatment both in the editorial office and in production. A Rapid Communication in Physical Review B may be no longer than four printed pages and must be accompanied by an abstract. Page proofs are sent to authors.*

#### Tunable two-dimensional photonic crystals using liquid-crystal infiltration

S. W. Leonard, J. P. Mondia, H. M. van Driel, O. Toader, and S. John

*Department of Physics, University of Toronto, 60 St. George Street, Toronto, Ontario M5S 1A7, Canada*

K. Busch

*Institute for Theory of Condensed Matter, University of Karlsruhe, P.O. Box 6980, D-76128 Karlsruhe, Germany*

A. Birner and U. Gösele

*Max-Planck-Institute of Microstructure Physics, Weinberg 2, D-06120 Halle, Germany*

V. Lehmann

*Infineon Technologies AG, Corporate Technology, Otto-Hahn-Ring 6, D-81730 München, Germany*

(Received 30 September 1999)

The photonic band gap of a two-dimensional photonic crystal is continuously tuned using the temperature dependent refractive index of a liquid crystal. Liquid crystal *E7* was infiltrated into the air pores of a macroporous silicon photonic crystal with a triangular lattice pitch of  $1.58\ \mu\text{m}$  and a band gap wavelength range of  $3.3\text{--}5.7\ \mu\text{m}$ . After infiltration, the band gap for the H polarized field shifted dramatically to  $4.4\text{--}6.0\ \mu\text{m}$  while that of the E-polarized field collapsed. As the sample was heated to the nematic-isotropic phase transition temperature of the liquid crystal ( $59\ ^\circ\text{C}$ ), the short-wavelength band edge of the H gap shifted by as much as  $70\ \text{nm}$  while the long-wavelength edge was constant within experimental error. Band structure calculations incorporating the temperature dependence of the liquid crystal birefringence can account for our results and also point to an escaped-radial alignment of the liquid crystal in the nematic phase.

Throughout the past decade, there has been a great deal of interest in photonic crystals (PCs), which are periodic dielectric materials capable of inhibiting the propagation of light over a spectral region known as a photonic band gap.<sup>1,2</sup> Following initial theoretical predictions, many crystals were fabricated, first in the microwave regime and recently in the visible regime. Many applications of PCs have been proposed including spontaneous emission control,<sup>2</sup> lasers,<sup>3</sup> waveguides, filters,<sup>4</sup> and optical limiters.<sup>5</sup> These applications would be significantly enhanced if the band structure of the crystal could be tuned. A practical scheme for tuning the band gap was recently proposed by Busch and John,<sup>6</sup> who showed that coating the surface of an inverse opal structure with a liquid crystal could be used to continuously tune the band gap. A step towards this goal was realized by Yoshino *et al.*,<sup>7</sup> who tuned the [111] stop band of an artificial opal

using the temperature dependent refractive index of a nematic liquid crystal.

In this paper, we report a tunable two-dimensional macroporous silicon PC possessing a photonic *band gap*, where the tuning of the band gap is achieved via the temperature dependent refractive index of a liquid crystal infiltrated into the pores. Upon heating the liquid crystal from the nematic to the isotropic phase, we observed a wavelength shift of  $70\ \text{nm}$  for the short-wavelength band edge (commonly referred to as the air band edge) in the  $\Gamma$ - $K$  direction. The long-wavelength band edge (the dielectric band edge) did not change within experimental error. Calculations based on a plane wave expansion method are consistent with the observed temperature dependence and suggest an escaped-radial alignment of the liquid crystal.

Two-dimensional PCs, possessing a triangular lattice of air pores with a pitch of  $1.58\ \mu\text{m}$ , were fabricated in

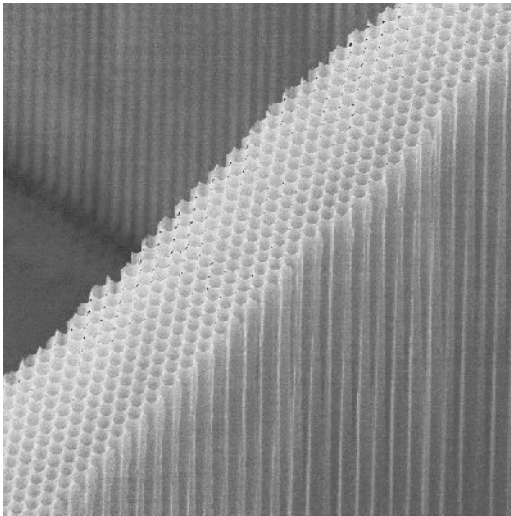


FIG. 1. Microstructured bar of macroporous silicon photonic crystal oriented in the  $\Gamma$ - $K$  direction with a width of 8 crystal layers.

macroporous silicon. The details of the fabrication process can be found in Ref. 8. A thin bar of a microstructured PC, with a width of 8 crystal rows and fixed on a silicon substrate, is shown in Fig. 1. Samples oriented in the  $\Gamma$ - $K$  direction with a height of 100  $\mu\text{m}$ , a length of 5 mm, and a width of 200  $\mu\text{m}$  (127 crystal rows) were prepared for this experiment.

The microstructured PCs were infiltrated with the liquid crystal *E7*, purchased from EM Industries Inc. The eutectic mixture *E7*, which is in the nematic phase at room temperature and undergoes a phase transition to the isotropic phase at 59  $^{\circ}\text{C}$ , was chosen for its wide nematic temperature range and large optical anisotropy of  $\Delta n = 0.2$ . In particular, the ordinary and extraordinary refractive indices at a temperature of 35  $^{\circ}\text{C}$  (deep in the nematic phase) and at a wavelength of 10.6  $\mu\text{m}$  are 1.49 and 1.69, respectively.<sup>9</sup> The infiltration was performed by submerging the PC sample into a small volume of *E7* heated well into the isotropic phase, utilizing the strong capillary action of the pores to draw up the liquid crystal.

The infiltrated samples were clamped between two brass plates, each of dimensions 1"  $\times$  1"  $\times$  1/8", in order to prohibit the leakage of light above the bar and below the substrate (the edges of the substrate were coated with silver paint). Small 1"  $\times$  1" kapton heaters were fixed to one face of each brass plate, and surface thermocouples were fixed to the opposite faces. The surface temperature of the brass plates was maintained using a temperature controller. Using this arrangement, the average temperature of the sample could be controlled within 0.2  $^{\circ}\text{C}$ , with an absolute accuracy of  $\pm 0.5$   $^{\circ}\text{C}$ . The transmission spectrum was measured using a Bomem MB Fourier transform infrared spectrometer, equipped with a mercury-cadmium-telluride detector and a mid-IR wire-grid polarizer.

The H-polarized transmission spectrum (i.e., with the  $E$ -field polarized perpendicular to the pore axes) of the un-infiltrated PC, oriented in the  $\Gamma$ - $K$  direction, is shown in Fig. 2(a). There is a wide stop band from 3.3–5.7  $\mu\text{m}$ . After infiltration, the transmission spectrum changes dramatically as shown in Fig. 2(b). The spectrum shows a stop band span-

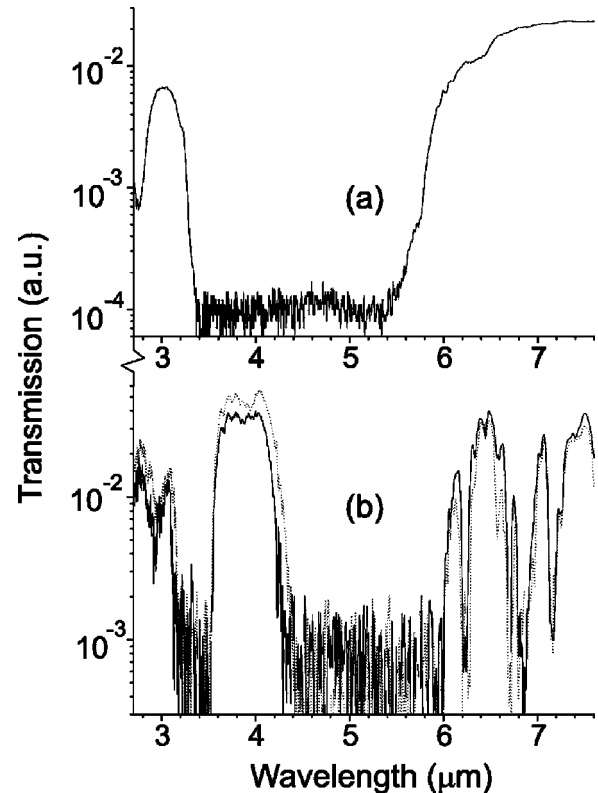


FIG. 2. H-polarized transmission spectrum of photonic crystal oriented in the  $\Gamma$ - $K$  direction (a) prior to and (b) after infiltration with liquid crystal *E7*. Solid line: nematic phase (35  $^{\circ}\text{C}$ ). Dotted line: isotropic phase (62  $^{\circ}\text{C}$ ).

ning a range of 4.4–6.0  $\mu\text{m}$ . The transmission minima at wavelengths of 3.4–3.5, 6.2, 6.7, 6.8, and 7.2  $\mu\text{m}$  are due to liquid crystal absorption lines. The sharpness of the band edges indicates complete infiltration. Although the H-polarized band gap remains open and large, the complete two-dimensional band gap of the original crystal has been lost due to the closing of the  $E$ -polarized band gap. The air band edge at 4.3  $\mu\text{m}$  shifts 70 nm upon heating the infiltrated sample to make the liquid crystal phase change from nematic to isotropic. The shorter-wavelength band edge at 3.2  $\mu\text{m}$  experiences a similar frequency shift. However, the dielectric band edge at 6  $\mu\text{m}$  has not shifted by any measurable amount. The air band edge wavelength is plotted as a function of temperature in Fig. 3. A measure of the band edge wavelength was obtained by taking the wavelength of the 3 dB point with respect to transmission peak at the band edge. As the temperature is increased, the band edge wavelength is redshifted until the phase transition from the nematic to the isotropic phase occurs. The disagreement between the accepted transition temperature of 59  $^{\circ}\text{C}$  and the measured temperature of  $60.5 \pm 0.5$   $^{\circ}\text{C}$  is attributed to a small ( $\sim 1$   $^{\circ}\text{C}$ ) vertical temperature differential across the sample, shifting the observed transition to a higher temperature.

In order to investigate the magnitude and direction of the observed band edge shift, calculations of the band structure of the infiltrated photonic crystal were performed using a plane wave expansion method. The refractive index for the H-polarized field depends on the alignment of the liquid crystal director field inside the pores. For simplicity, we chose to model an axial alignment, in which the liquid crys-

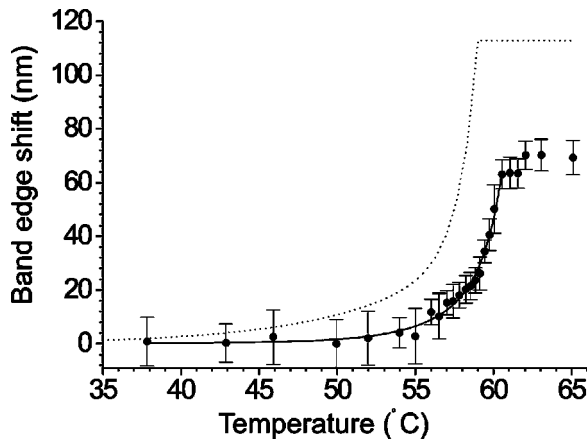


FIG. 3. Dependence of wavelength shift of air band edge on temperature of infiltrated photonic crystal. Solid line: fit to data. Dashed line: calculations based on axial director alignment.

tal director is parallel to the pore axis. The pore is therefore uniaxial, with the optic axis being in the direction of the pore axis. In this case, the H-polarized field becomes an ordinary ray, and the refractive index within the pore is  $n_0$ . Calculations of the H-polarized band structure were made using refractive index values of  $n_0$  measured at a wavelength of  $10.6 \mu\text{m}$ ,<sup>9</sup> ranging from 1.489 at  $35^\circ\text{C}$  to 1.541 at  $59^\circ\text{C}$  [the difference between  $n_0(10.6 \mu\text{m})$  and  $n_0(4 \mu\text{m})$  is expected to be less than 0.3% based on the extrapolation of measurements of  $n_0$  made in the visible regime]. The refractive index of silicon at a wavelength of  $5 \mu\text{m}$  was taken to vary between 3.428 ( $35^\circ\text{C}$ ) and 3.432 ( $65^\circ\text{C}$ ), in agreement with Ref. 10.

The results of the calculations are also shown in Fig. 3, where the air band edge wavelength is plotted as a function of temperature for the  $\Gamma$ - $K$  direction (the frequency shift is constant across the entire Brillouin zone boundary). Comparing these results with the data, one observes that although the band edge is shifting in the same direction for both cases, the calculated shift of 113 nm is much larger than the experimental value of 70 nm.

The fact that the experimental and theoretical shifts are in the same direction indicates that the actual alignment is largely axial. However, the lack of evidence of a complete axial shift in the experimental data suggests a more complicated director field. The director field of a liquid crystal in a porous medium is strongly dependent on the interplay between the elastic properties of the liquid crystal and the nature of the anchoring at the pore wall.<sup>11</sup> The two anchoring types are homeotropic, where the liquid crystal molecules align perpendicular to the pore wall, and homogeneous, where the alignment is parallel to the pore wall. The type and strength of surface anchoring of *E7* in macroporous silicon has not yet been identified. If we assume homeotropic alignment of the liquid crystal, as was the case for pentylcyanobiphenyl (5CB) nematic liquid crystal in a silica aerogel matrix,<sup>12</sup> then the potential director fields are axial (AX), escaped-radial (ER) (possibly accompanied by point defects) and planar-polar (PP) configurations. The ER configuration occurs when the director, which is anchored homeotropically at the pore wall, escapes into the third dimension towards the center of the pore. The PP configuration occurs when the

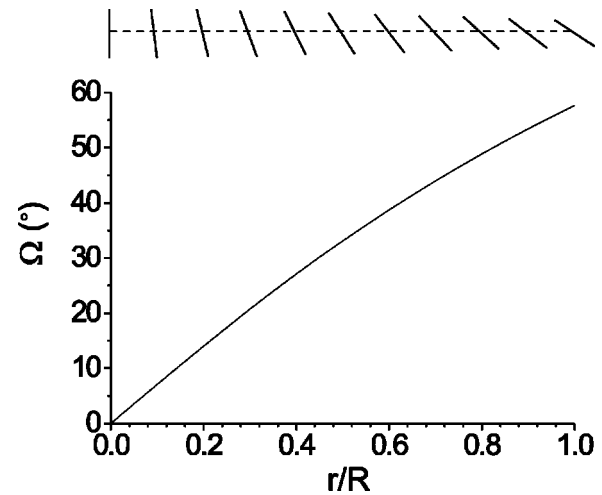


FIG. 4. Alignment of liquid crystal within cylindrical pore for the case of escaped-radial configuration with a weak molecular anchoring strength of  $W_\theta = 1 \times 10^{-5} \text{ J/m}^2$ . Bottom: radial dependence of director angle  $\Omega$ . Top: orientation of director at discrete radial points.

director field remains in the plane perpendicular to the pore axis forming a polar distribution.

The stability of a particular configuration can be analyzed by calculating the free energy. The free energy per unit pore length of the AX, ER and PP configurations can be found in Table 1 of Ref. 13. Using the Frank elastic constants of  $E7$ ,  $K_{11} = 11.1 \text{ pN}$ ,  $K_{33} = 17.1 \text{ pN}$ , and  $K_{24} = 28.6 \text{ pN}$ ,<sup>14</sup> one finds that the ER configuration is stable over that of the AX and PP configurations for all molecular anchoring strengths  $W_\theta$ .<sup>13</sup>

The director field for the ER configuration, given by the angle  $\Omega(r)$  between the local director and the pore axis, can be obtained by solving the implicit equation<sup>15,13</sup>

$$\frac{r}{R} = \sqrt{\frac{(\sigma+1)(\Delta-1)}{(\sigma-1)(\Delta+1)}} \exp\left(\sqrt{\eta-1} \arctan \frac{\sqrt{\eta-1}(\Delta-\sigma)}{\Delta\sigma+\eta-1}\right), \quad (1)$$

where  $R$  is the pore radius,  $r$  is the radial coordinate within the pore,  $\sigma = W_\theta R / K_{11} + K_{24} / K_{11} - 1$ ,  $\Delta = \sqrt{1 + \eta \tan^2 \Omega(r)}$  and  $\eta = K_{33} / K_{11}$ . A particular realization of the ER configuration for a weak molecular anchoring strength of  $W_\theta = 1 \times 10^{-5} \text{ J/m}^2$  is shown in Fig. 4, where  $\Omega$  is plotted as a function of  $r$  and the orientation of the director is shown above the graph. The director is axially aligned at the pore center ( $r=0$ ) and rotates as a function of radius to an angle of  $58^\circ$  at the pore wall ( $r=R$ ). In this case, the H-polarized light experiences the spatially averaged refractive index within the pore which is larger than  $n_0$  and increases with temperature until the nematic-isotropic phase transition occurs. The resulting smaller wavelength shift is consistent with the observations. It would be useful to unambiguously determine the anchoring type and director alignment using nuclear magnetic resonance techniques.<sup>16,17</sup>

The calculations (based on the AX configuration) also predict a wavelength shift of 51 nm for the dielectric band edge over a temperature range of  $35$ – $62^\circ\text{C}$ . The difference between this shift and the larger shift of 113 nm for the air band edge is a result of the different spatial electromagnetic

field distributions of the two bands. The dielectric band is a mode with most of its energy propagating in the high dielectric material.<sup>18</sup> Orthogonality between modes causes the air band to have the majority of its field energy propagating in the low dielectric material. Therefore, the air band is much more sensitive to changes in the dielectric constant of the low-dielectric medium (i.e., the liquid crystal). Furthermore, the spatial distribution of the field within the pore plays an important role in determining the magnitude of the tuning shift. In the case of the air band, calculations show that the electric field is concentrated near the pore center and decreases towards the pore wall. Thus the field is most sensitive to the director alignment near the pore center, which is largely axial in the case of the ER configuration. On the other hand, the electric field within the pore for the dielectric band is large near the pore wall and decreases to a very small amplitude at the pore center. This mode is therefore most sensitive to the director alignment near the pore wall. In the vicinity of the pore wall, the ER director is tilted at a large angle with respect to the pore axis (the amount of tilt depending on the anchoring strength  $W_\theta$ ). The refractive index in this region will be a complicated spatial average of  $n_0$  and  $n_e$  (the extraordinary refractive index), where the averaging is dependent on the director alignment, the field amplitude, and the polarization. This averaged value will change by a smaller amount than  $n_0$  as the liquid crystal is heated from the nematic to the isotropic phase. Therefore, the lack of an experimentally observed shift for the dielectric band is also consistent with an ER director configuration.

Although the tuning range is a relatively small percentage of the band gap (3%), it is large enough to broadly tune the narrow spectral features characteristic of many PC applications, e.g., filters, microcavities, waveguides and lasers. Of course, the tuning could also be used to close the band gap provided that the band gap was sufficiently small. For the case of the *E*-polarized field, the tuning range would be

larger since the extraordinary refractive index changes by a greater amount than the ordinary refractive index from the nematic to the isotropic phase. Even though the *E*-polarized band gap between the second and third bands was closed after infiltration, calculations predict the existence of another band gap between the seventh and eighth bands (at a wavelength of 2.3  $\mu\text{m}$ ) that could be tuned in this manner. The switching time of liquid crystal infiltrated PC devices could be decreased to times on the order of 10 ms (Ref. 19) using electric fields to reorient the director field. The *n*-type silicon samples used in this experiment, however, contained a high density of free carriers ( $<10^{17} \text{ cm}^{-3}$ ) that would screen an applied electric field.

In summary, we have demonstrated the first tunable photonic band gap using liquid crystals infiltrated into a two-dimensional macroporous silicon PC. The wavelength of the H-polarized air band edge (in the  $\Gamma$ -*K* direction) was continuously tuned over 70 nm by raising the temperature of the infiltrated liquid crystal from the nematic to the isotropic phase. Band structure calculations based on an axial alignment of the liquid crystal predicted a shift of 113 nm. The measured shift, which is smaller yet in the same spectral direction, is consistent with the interpretation that the liquid crystal is aligned in an escaped-radial configuration. The results highlight the possibility of significantly enhancing the properties of many photonic crystal applications and also provide an alternative probe of liquid crystal alignment and phase transitions in confined geometries.

The authors would like to thank F. Allen, D. Finotello, and E. Kumeacheva for helpful suggestions. Part of this work was funded by the Natural Sciences and Engineering Research Council of Canada and Photonics Research Ontario, for which S.W.L., J.P.M., H.M.v.D., O.T. and S.J. are grateful. Financial support by the Deutsche Forschungsgemeinschaft (projects GO 704/2-1 and Bu 1107/1-1) is gratefully acknowledged by A.B. and K.B.

- 
- <sup>1</sup>S. John, Phys. Rev. Lett. **58**, 2486 (1987).  
<sup>2</sup>E. Yablonovitch, Phys. Rev. Lett. **58**, 2059 (1987),  
<sup>3</sup>K. Inoue, M. Sasada, J. Kawamata, K. Sakoda, and J.W. Haus, Jpn J. Appl. Phys., Part 2 **38**, L157 (1999).  
<sup>4</sup>R.D. Meade, A. Devenyi, J.D. Joannopoulos, O.L. Alerhand, D.A. Smith, and K. Kash, J. Appl. Phys. **75**, 4753 (1994).  
<sup>5</sup>H-B. Lin, R. Tonucci, and A.J. Campillo, Opt. Lett. **23**, 94 (1998).  
<sup>6</sup>K. Busch and S. John, Phys. Rev. Lett. **83**, 967 (1999).  
<sup>7</sup>K. Yoshino, Y. Shimoda, Y. Kawagishi, K. Nakayama, and M. Ozaki, Appl. Phys. Lett. **75**, 932 (1999).  
<sup>8</sup>S.W. Leonard, H.M. van Driel, K. Busch, S. John, A. Birner, A.-P. Li, F. Müller, U. Gösele, and V. Lehmann, Appl. Phys. Lett. **75**, 3063 (1999).  
<sup>9</sup>I.C. Khoo, J. Mod. Opt. **37**, 1801 (1990).  
<sup>10</sup>H.H. Li, J. Phys. Chem. Ref. Data **9**, 561 (1980).  
<sup>11</sup>G.P. Crawford and S. Žumer, in *Liquid Crystals in Complex Geometries Formed by Polymer and Porous Networks*, edited by G.P. Crawford and S. Žumer (Taylor & Francis Ltd., London, 1996), Chap. 1.  
<sup>12</sup>S. Kralj, G. Lahajnar, A. Zidanšek, N. Vrbancič-Kopač, M. Vilfan, R. Blinc, and M. Kosec, Phys. Rev. E **48**, 340 (1993).  
<sup>13</sup>S.V. Burylov, JETP **85**, 873 (1997).  
<sup>14</sup>R.D. Polak, G.P. Crawford, B.C. Kostival, J.W. Doane, and S. Žumer, Phys. Rev. E **49**, R978 (1994).  
<sup>15</sup>G.P. Crawford, D.W. Allender, and J.W. Doane, Phys. Rev. A **45**, 8693 (1992).  
<sup>16</sup>G.P. Crawford, M. Vilfan, J.W. Doane and I. Vilfan, Phys. Rev. A **43**, 835 (1991).  
<sup>17</sup>G.P. Crawford, D.W. Allender, J.W. Doane, M. Vilfan, and I. Vilfan, Phys. Rev. A **44**, 2570 (1991).  
<sup>18</sup>J.D. Joannopoulos, R.D. Meade, and J.N. Winn, *Photonic Crystals: Molding the Flow of Light* (Princeton University Press, Princeton, 1995).  
<sup>19</sup>H.-S. Kitzerow, in *Liquid Crystals in Complex Geometries Formed by Polymer and Porous Networks*, edited by G.P. Crawford and S. Žumer (Taylor & Francis Ltd., London, 1996), Chap. 8.